miR-214 ameliorates sepsis-induced acute kidney injury via PTEN/AKT/mTOR-regulated autophagy

ZHENZHEN SANG[1], SHIMIN DONG[2*], PU ZHANG[2*] and YUNXIA WEI[2*]

[1]Emergency Department, Cangzhou Central Hospital, Cangzhou, Hebei 061001; [2]Department of Emergency, The Third Hospital of Hebei Medical University, Shijiazhuang, Hebei 050000, P.R. China

Received December 22, 2020; Accepted June 29, 2021

DOI: 10.3892/mmr.2021.12322

Abstract. Previous studies have suggested that oxidative stress and autophagy results in acute kidney injury (AKI) during sepsis and microRNA (miR)-214 serves a vital role in the protection of kidneys subjected to oxidative stress. The present study aimed to test whether the renoprotection of miR-214 is related to autophagy in sepsis. The role of autophagy was investigated in a mouse model of cecal ligation and puncture (CLP). Reverse transcription-quantitative polymerase chain reaction (RT-qPCR) was used to analyze the expression of miR-214. The structure and function of kidneys harvested from the mice were evaluated. Kidney autophagy levels were detected with immunohistochemical, immunofluorescent and western blotting. It was found that miR-214 could alleviate AKI in septic mice by inhibiting the level of kidney autophagy. Furthermore, miR-214 inhibited autophagy by silencing PTEN expression in the kidney tissues of septic mice. These findings indicated that miR-214 ameliorated CLP-induced AKI by reducing oxidative stress and inhibiting autophagy through the regulation of the PTEN/AKT/mTOR pathway.

Introduction

Acute kidney injury (AKI) is one of the most common complications of sepsis and occurs in 40-50% of septic patients, with a mortality rate of as high as 60% (1). However, the pathogenesis of sepsis-induced AKI remains unclear. Autophagy has been reported to serve a key role in sepsis-induced AKI and the inhibition of autophagy results in the development of AKI during sepsis (2,3). Previous studies (4,5) have confirmed that sepsis triggers autophagy in multiple organs, including the kidney (6) and autophagic processes are involved in the removal of damaged mitochondria and oxidative stress (7). However, excessive autophagy can cause unwanted and deleterious cell death (8). Therefore, a moderate level of autophagy is the key to reducing sepsis-induced AKI. Previous studies have reported that miR-214 ameliorates ischemia-reperfusion-induced AKI by inhibiting apoptosis (9) and miR-214 suppresses oxidative stress in diabetic nephropathy via the reactive oxygen species (ROS)/AKT/mTOR signaling pathway (10). The present study found that miR-214 can attenuate sepsis-induced myocardial dysfunction in mice by inhibiting autophagy (11). However, whether miR-214 can ameliorate sepsis-induced AKI remains to be elucidated. In present study, it was hypothesized that miR-214 attenuates CLP-induced AKI by reducing oxidative stress and inhibiting autophagy through the regulation of the PTEN/AKT/mTOR pathway.

Materials and methods

Animals. A total of 100 Kunming male mice (weight, 20.40±2.92 g; age, 6-8 weeks) supplied by the Medical Laboratory Animal Centre of the Hebei Medical University (Shijiazhuang, China) were used in the present study. All mice were acclimated to a 12-h light/dark cycle at 24˚C with 50% humidity and were given free access to food and water at ≥1 week before the experiments. All the experimental procedures were performed in strict accordance with the National Institute of Health guidelines (NIH Publication No 85-23, revised 1996) and approval by the Institutional Animal Care and Use Committees of the Cangzhou Central Hospital (approval no. 2017-020-01). All surgeries were performed under anesthesia and every effort was made to minimize suffering.

Cecal ligation and puncture (CLP). CLP was performed on mice to create a murine sepsis model, as previously described (12). Following anesthetizing by isoflurane inhalation (induced at 3% and maintained at 0.5%), a 1 cm midline incision was cut. The exposed cecum (1 cm distance from the end) was ligated with two punctures using a 23-gauge needle. The cecum gently extruded a small amount of feces and was placed back in its anatomical position. The abdominal wall was sutured in layers with a 3-0 silk braid. Following the procedure, 1 ml of 0.9% saline was injected subcutaneously. The mice were provided free access to only water. Sham

Correspondence to: Dr Zhenzhen Sang, Emergency Department, Cangzhou Central Hospital, 16 Xinhua Road, Yunhe Qu, Cangzhou, Hebei 061001, P.R. China
E-mail: szz15383178125@hotmail.com

*Contributed equally

Key words: microRNA-214, sepsis, acute kidney injury, autophagy

model mice were operated in the same manner as the CLP model without CLP.

Experimental design. Mice (n=6 for sham surgery and CLP) were randomly assigned to seven groups: Sham group, CLP group, adenovirus (Ad)-green fluorescent protein (GFP) + CLP group, Ad-miR-214 + CLP group, anti-miR-214 + CLP group, PTEN inhibitor + CLP group and Ad-miR-214 + PTEN inhibitor + CLP group. The Sham group mice were exposed to the same procedure but without ligation and puncture of the cecum. Mice in the other groups received cecal ligation and perforation. All mice were quickly anesthetized by isoflurane inhalation to collect blood, urine and kidney samples 24 h after the last treatment.

Adenovirus-mediated Ad-miR-214, anti-miR-214, or Ad-GFP gene transfer in vivo and PTEN inhibitor injection. Ad-miR-214, anti-miR-214, or Ad-GFP (Shanghai GenePharma Co., Ltd.) was delivered into the abdominal cavity of mice 4 days prior to CLP. Briefly, mice were anesthetized by isoflurane inhalation. A catheter containing 200 μl of adenovirus ($2x10^{11}$ pfu, expressing miR-214, anti-miR-214, or Ad-GFP) was administered to normal mice via intraperitoneal injection. The PTEN inhibitor (VO-OHpic, intraperitoneal, Sigma-Aldrich; Merck KGaA) was administered to CLP mice that had received anti-miR-214 via intraperitoneal injection at a single dosage of 10 μg/kg 30 min prior to the administration of adenovirus.

Assessment of kidney function. Blood samples were harvested from mice heart, followed by centrifugation (at room temperature for 15 min at 3,000 x g) for collecting serum. The serum levels of blood urea nitrogen (BUN) and serum creatinine (Cr) were determined using a Hitachi 7600 automatic analyzer (Hitachi, Ltd.). ELISA was used to analyze levels of kidney injury molecule-1 (KIM-1; cat. no. RKM100; R&D Systems, Inc.) and neutrophil gelatinase-associated lipocalin (NGAL; cat. no. DY3508; R&D Systems, Inc.) in urine samples.

Assay for serum inflammation cytokine. Serum TNF-α (cat. no. H052) and IL-6 (cat. no. H007) were examined using commercial ELISA kits (Nanjing Jiancheng Bioengineering Institute) according to the manufacturer's instructions.

Measurement of oxidative stress markers. The corresponding assay kit (Nanjing Jiancheng Bioengineering Institute, Nanjing, China) was used to measure the levels of malondialdehyde (MDA) and test the activity of superoxide dismutase (SOD) in accordance with the manufacturer's instructions.

Histology and tubular injury score. All mice were subjected to kidney perfusion under anesthesia 24 h after CLP. The kidney specimens were fixed in 4% paraformaldehyde for 72 h at 4˚C. The tissue samples were then dehydrated in a graded series of ethanol solutions, embedded in paraffin and cut into 4-μm sections. Sections (4 μm) were cut using a microtome and the tissue sections were stained with hematoxylin (5 min) and eosin (1 min) at room temperature for histological examination. The slides were evaluated and graded using a microscope (BX51, Olympus Corporation). Renal tissues with the following histopathological changes were judged injured: Loss of brush border, vacuolization, cast formation, tubular dilation and disruption, cell lysis and cellular necrosis. Tissue damage was checked in a blinded manner and scored by the percentage of damaged tubules: 0, no damage; 1, 0-25; 2, 25-50; 3, 50-75; 4, >75% (13).

Transmission electron microscopy (TEM). Fresh kidneys were washed in phosphate buffered saline, and cut into 1 mm cubes and sequentially fixed in 2.5% glutaraldehyde for 24 h at 4˚C. The sections were immersed in 1% osmium tetroxide for 2 h at 4˚C, dehydrated in graded ethanol and embedded in epoxy resin. Finally, the ultrathin sections (60 nm) were doubled stained with uranyl acetate and lead citrate at 20˚C for 60 min. The observation was performed on a transmission electron microscope (Tecnai; Hitachi, Ltd.) at 80 kV using Electron Microscopy Film 4489 (ESTAR thick base; Kodak).

Immunohistochemistry (IHC). Fresh kidney tissues were fixed in 4% paraformaldehyde (for 72 h at 4˚C) and embedded in paraffin. Specimens were cut into 4 μm-thick sections and deparaffinized in xylene. After tissue sections were washed with PBS, they were boiled in 10 mM citrate buffer (pH 6.0) for 4 min for antigen retrieval and then blocked with 10% goat serum in PBS at room temperature for 1 h. The primary antibody (anti-LC3B; 1:400; cat. no. 4412; Cell Signaling Technology, Inc.) was added in accordance with the instructions and incubated at 4˚C for 12 h. The secondary antibody (goat antirabbit HRP; 1:2,000; cat. no. BS13278; Bioworld Technology, Inc.) was added and incubated at room temperature for 10 min. DAB (100 μl) was added and counterstained for 5 min with the staining observed under a light microscope (Model CX31-P; Olympus Corporation). The intensity of positive staining, which appeared brown, was determined using Image-Pro Plus 6.0 image analysis software (Media Cybernetics, Inc.). The integral optical density (IOD) was calculated to represent the intensity. IOD values increased as protein expression increased.

Reverse transcription-quantitative (RT-q) PCR. Total RNA was extracted from kidney tissue following the induction of the model using TRIzol reagent (Thermo Fisher Scientific, Inc.). According to the instructions of the TaqMan reverse transcription kit (cat. no. N8080234; Invitrogen; Thermo Fisher Scientific, Inc.), RNA was reverse transcribed into cDNA. The following thermocycling conditions were used (miR-214): Initial denaturation at 95˚C for 5 min; followed by 40 cycles of denaturation at 95˚C for 30 sec, annealing at 60˚C for 30 sec and elongation at 72˚C for 30 sec. RT-qPCR was performed using an ABI Prism 7500 Sequence Detection System (PerkinElmer, Inc.) and a standard SYBR Green PCR kit (Toyobo Life Science). U6 was used as the internal control for miR-214. Primer sequences were as follows: miR-214, forward, 5'-AGCATAATACAGCAGGCACAGAC-3' and reverse, 5'-AAAGGTTGTTCTCCACTCTCTCAC-3'; U6, forward, 5'-ATTGGAACGATACAGAGAAGATT-3' and reverse, 5'-GGAACGCTTCACGAATTTG-3'. These experiments were replicated six times. Results were analyzed using the $2^{-\Delta\Delta Cq}$ method (14). The mRNA expression levels of LC3, p62, PTEN, AKT and mTOR were evaluated via RT-qPCR. With β-actin as an internal reference of these genes, the $2^{-\Delta\Delta Cq}$

Table I. Primer sequences for reverse transcription-quantitative PCR.

Gene	Sequence
miR-214-3p	F: 5'-GTCGTATCCAGTGCAGGGTCCGAGGTATTCGCACTGGATACGACACTGCC-3'
	R: 5'-GCACAGCAGGCACAGACA-3'
PTEN	F: 5'-CACAGAATTCCAGACATGACAGCCATCATC-3'
	R: 5'-GTGGATCCTCTAGGTTTATCCCTCTTG-3'
mTOR	F: 5'-AACAACGGCTTTCCACCAGG-3'
	R: 5'-CACCCTAAGTGAGCCCTTGGA-3'
AKT	F: 5'-CCACGCACACTCGGGCCG-3'
	R: 5'-CAATGCAGAGGGGTGCAGG-3'
LC3	F: 5'-CATGCCGTCCGAGAAGACCT-3'
	R: 5'-GATGAGCCGGACATCTTCCACT-3'
p62	F: 5'-TCCCTGTCAAGCAGTATCC-3'
	R: 5'-TCCTCCTTGGCTTTGTCTC-3'
U6	F: 5'-CTCGCTTCGGCAGCACA-3'
	R: 5'-AACGCTTCACGAATTTGCGT-3'
β-actin	F: 5'-ACACTGTGCCCATCTACGAGG-3'
	R: 5'-AGGGGCCGGACTCGTCATACT-3'

was used to measure the relative expression of target genes. The primer sequences shown in Table I were synthesized by Sangon Biotech Co., Ltd.

Western blotting. Kidney tissue was mixed with RIPA lysate (Beyotime Institute of Biotechnology) to make the homogenate and lysis was stopped when no visible tissue was observed. The samples were centrifuged at 13,000 x g for 10 min at -4˚C and the supernatant was recovered for the western blot analysis. In brief, protein concentrations were determined using the micro BCA protein assay kit (Thermo Fisher Scientific, Inc.). Protein samples (80 μg per sample) were subjected to separate by reducing 12% sodium dodecyl sulfate-polyacrylamide gel electrophoresis and then transferred onto polyvinylidene difluoride membranes at 4˚C overnight. Separated proteins were transferred to PVDF membranes. Following blocking in 5% skimmed milk at room temperature for 2 h, membranes were incubated overnight (at 4˚C) with primary antibodies. The following primary antibodies (all Cell Signaling Technology, Inc.) were used: Light chain 3B (1:1,000; cat. no. 4412), p62 (1:1,000; cat. no. 4412), Anti-PTEN (1:1,000; cat. no. 9188), anti-phosphorylated (p)-AKT (Ser473) (1:1,000; cat. no. 4060), anti-AKT (1:1,000; cat. no. 9272), anti-p-mTOR (Ser 2448) (1:1,000; cat. no. 5536), anti-mTOR (1:1,000; cat. no. 2972) and β-actin (1:2,000; cat. no. 4970). After washing, the membranes were incubated (at room temperature for 2 h) with the HRP-conjugated anti-rabbit secondary antibodies (1:3,000; cat. no. A0208; Beyotime Institute of Biotechnology). Protein bands were detected with Immobilon Western (MilliporeSigma) and analyzed using Total-Lab TL120 software (Nonlinear Dynamics, 2.01). The expression of protein was normalized to β-actin.

Statistical analysis. Statistical analysis was performed using the GraphPad Prism 9.0 (GraphPad Software, Inc.). All data were presented as means ± standard deviation or medians (interquartile ranges) for continuous variables, depending on their distributions. Baseline characteristics and outcomes were compared using one-way ANOVA followed by Tukey's post hoc test, or Kruskal-Wallis test followed by Dunn's test as appropriate. $P<0.05$ was considered to indicate a statistically significant difference.

Results

Time point 24 h after CLP. Previous studies have reported (6,15,16) that biochemical (i.e., LC3 and p62) analysis reveals that autophagy flux is suppressed with progression of sepsis following 6-8 h of CLP. In the present study, the number of autolysosomes in the kidney of CLP-treated mice increased within 24 h following surgery. In addition, the analysis of markers of kidney injury showed that renal function was most seriously damaged 24 h after CLP. Therefore, the time point 24 h after CLP was choose for the following experiments.

Regulatory effect on miR-214 in kidney tissues. RT-qPCR analysis was used to detect miR-214 expression in CLP-treated mice. It was found that miR-214 expression was slightly upregulated in the kidney tissues following CLP surgery 24 h, as compared with the sham group (1.47-fold, $P<0.01$, Fig. 1A). The present study examined the reactive increase in miR-214 expression during sepsis as a compensatory protective mechanism. Therefore, it evaluated the role of miR-214 in AKI during sepsis by regulating its expression. As shown in Fig. 1B, Ad-miR-214 increased miR-214 expression by 4.13-fold 4 days after intraperitoneally injecting $2x10^{11}$ pfu/mice adenovirus, whereas anti-miR-214 decreased miR-214 expression by 81.16% in the kidney tissue, as compared with the sham group (both $P<0.01$). By contrast, Ad-GFP as a control group did not affect miR-214-3p expression, compared with the sham group (both $P>0.05$).

Effect of miR-214 on renal dysfunction in septic mice. All mice were sacrificed to collect blood, urine and kidney samples 24 h after the CLP surgery. BUN and Cr are important indicators of the severity of renal impairment (17). Furthermore, NGAL and KIM-1 have been identified as specific biomarkers of kidney injury and their increased expression is associated with early renal tubular injury in AKI (17). As shown in Fig. 2A-D, the levels of BUN, Cr, KIM-1 and NGAL were significantly increased following CLP surgery compared with the sham group. However, Ad-miR-214 significantly decreased BUN, Cr, KIM-1 and NGAL levels in comparison with the CLP group (all $P<0.01$), whereas anti-miR-214 exhibited opposite effects in these kidney function parameters. However, following pretreatment with PTEN inhibitor, the protection effects of Ad-miR-214 were enhanced. The results show that miR-214 attenuates kidney dysfunction in septic mice.

Effect of miR-214 on renal inflammation and oxidative stress. As shown in Fig. 3A and B, CLP significantly elevated the levels of TNF-α and IL-6, whereas Ad-miR-214 significantly decreased the levels of these markers. Compared with the

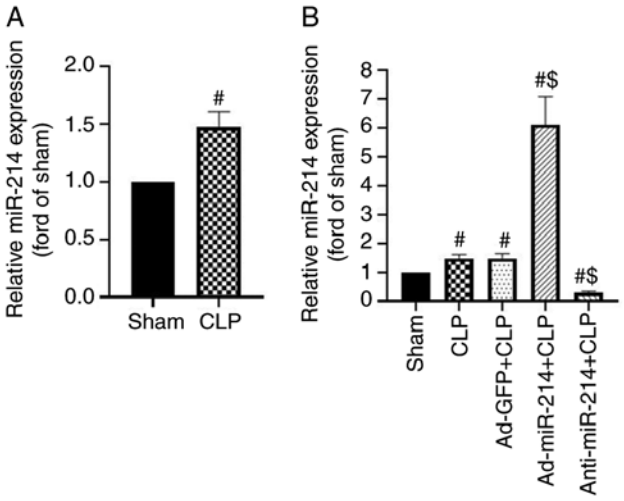

Figure 1. miR-214 expression levels detected by RT-qPCR reverse transcription-quantitative PCR. (A) CLP induced miR-214 upregulation in kidney tissues. (B) Modulation of miR-214 expression in kidney tissues. Ad-miR-214, anti-miR-214, or Ad-GFP was delivered into mice abdominal cavity 4 days prior to CLP. The miR-214 expression levels were determined via RT-qPCR. n=6; $^{\#}$P<0.01 vs. the sham group; $^{\$}$P<0.01 vs. CLP group. miR, microRNA; RT-qPCR, reverse transcription-quantitative PCR; CLP, cecal ligation and puncture; Ad, adenovirus.

Ad-GFP group, the levels of these inflammatory cytokines were significantly increased in the anti-miR-214 group, while can be reduced by Ad-miR-214. However, following pretreatment with PTEN inhibitor, the protection effects of Ad-miR-214 were enhanced. These results suggest that miR-214 can reduce the levels of inflammatory cytokines.

As shown in Fig. 3C and D, the CLP increased the levels of MDA and decreased the levels of SOD in comparison with the CLP group (both P<0.01). However, Ad-miR-214 significantly increased the levels of MDA and decreased levels of SOD in comparison with the CLP group (all P<0.01), whereas anti-miR-214 exhibited opposite effects in these oxidative stress parameters (both P<0.01). However, following pretreatment with PTEN inhibitor, the antioxidant effects of Ad-miR-214 were enhanced.

Effect of miR-214 on renal histopathological damage. As shown in Fig. 4, there were substantial pathological changes in the CLP group, which included edema of renal tubular epithelial cells (green arrow), tubular necrosis (blue arrow), telangiectasia and severe congestion/hemorrhage (red arrow). However, the CLP-induced kidney damage was significantly improved by pretreatment with Ad-miR-214. The damaging effect was enhanced by anti-miR-214.

Effect of miR-214 on renal ultrastructural changes. Fig. 5 shows that in the sham group, cells had an intact nuclear morphology and cell mitochondria exhibited normal morphology with clearly discernible cristae. In the CLP group, mitochondria defects were observed, such as swelling, disorganization, reduction or vanishing of the cristae and increasing mitophagy (white arrow) and autolysosomes (black arrow). Ad-miR-214 alleviated cell mitochondria injury and mitophagy, which were induced by CLP. Anti-miR-214 aggravated cell mitochondria injury and mitophagy, which were induced by CLP.

Effect of miR-214 on renal autophagy in septic mice. The present study examined the changes in LC3 in kidney tissues via IHC staining. As shown in Fig. 6, the LC3 intensity of positive staining increased significantly in the CLP group compared with the sham group (P<0.01) due to the activated autophagy. The expression level of LC3 was lower in the Ad-miR-214 group and higher in the anti-miR-214 group in comparison with the CLP group (P<0.01). However, the administration of PTEN inhibitor enhanced the inhibition of autophagy effect of Ad-miR-214.

miR-214 activates the AKT/mTOR pathway to inhibit autophagy by silencing PTEN in kidney tissues. The effect of CLP on autophagy in kidney tissues was investigated by assessing the levels of LC3-II/I and p62. The PTEN/AKT/mTOR signaling pathway serves an important role in autophagy (18). To investigate the effect of miR-214 on the PTEN-AKT/mTOR pathway, the protein levels of LC3-II/I, p62, AKT, p-AKT, mTOR, p-mTOR and PTEN were analyzed through western blotting and RT-qPCR analysis. As shown in Fig. 7A-C, modification in these proteins rapidly occurs, with an increase in the rate of LC3-II/LC3-I, and reduction in the levels of p62 (both P<0.01) in the CLP-induced sepsis group. Compared with the CLP group, the rate of LC3-II/LC3-I was significantly decreased, while the level of p62 (both P<0.01) was significantly increased in the Ad-miR-214 group. However, the inhibition of miR-214 displayed an opposite tendency to the above indicators (both P<0.01). By contrast, the negative control had no effect on the changes in the rate of LC3-II/LC3-I and the levels of p62 in kidney tissues (both P>0.05). The two indicators of LC3-II/LC3-I and p62 had no significant difference among the Ad-miR-214 group, the PTEN inhibitor group and the Ad-miR-214 + PTEN inhibitor group (all P>0.05). These results showed that autophagy was induced by CLP, and the overexpression of miR-214 could partially inhibit it.

As shown in Fig. 7A and D-F, the expression level of PTEN (P<0.01) was increased, and the expression levels of p-AKT (Ser473) and p-mTOR (Ser2448) (P<0.01) were decreased by CLP. Compared with the CLP group, the expression level of PTEN was reduced, while those of p-AKT and p-mTOR (all P<0.01) were subsequently increased in the Ad-miR-214 group. By contrast, the negative control had no effect on the changes in the expression levels of PTEN, p-AKT and p-mTOR in kidney tissues (all P>0.05). There was no significant difference in the above indicators among the Ad-miR-214 group, the PTEN inhibitor group and the Ad-miR-214 + PTEN inhibitor group (all P>0.05). These findings suggests that CLP induces kidney tissue autophagy by inhibiting the AKT/mTOR pathway. Ad-miR-214 activated the AKT/mTOR pathway by silencing PTEN in kidney tissues. However, compared with the CLP group, anti-miR-214 did not significantly inhibited the expression of mTOR. Therefore, RT-qPCR was further used to determine the expression of mRNA of genes related to the PTEN/AKT/mTOR signaling pathway. According to the results of RT-qPCR (Fig. 8), in comparison with the Sham group, the mRNA expression levels of p62, LC3 and PTEN were markedly increased, while the mRNA expression of AKT and mTOR were decreased in the CLP group. Compared with the CLP group, the Ad-miR-214, PTEN

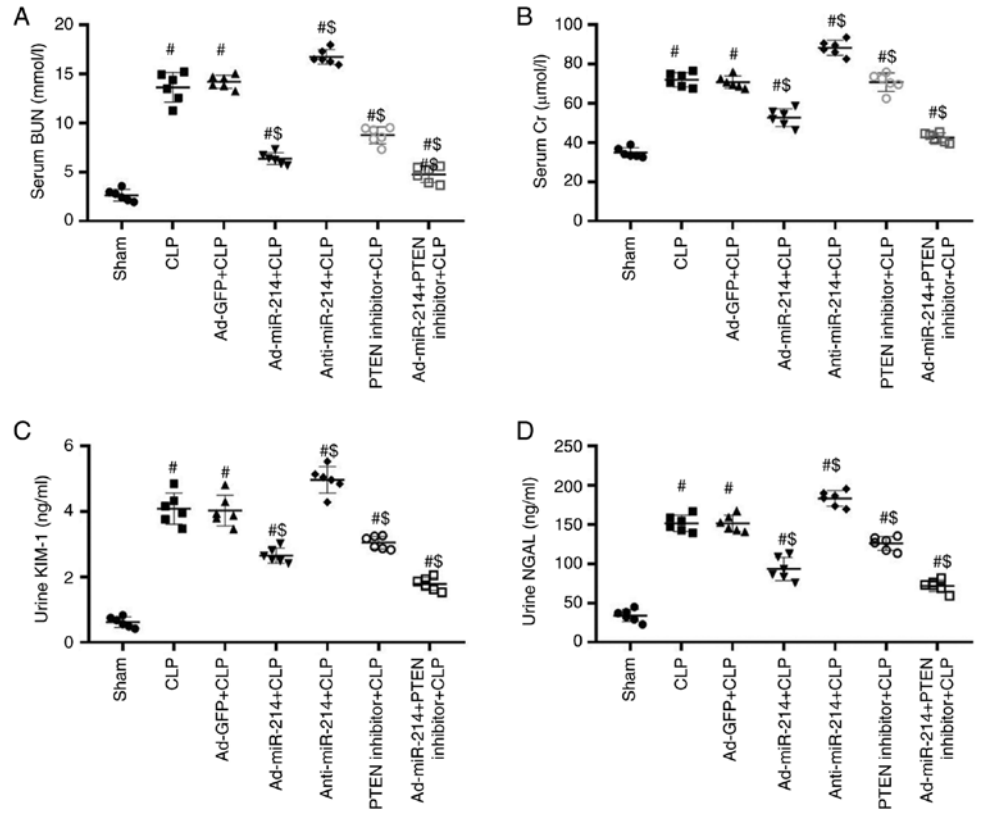

Figure 2. miR-214 improves renal dysfunction in CLP-induced AKI. (A) Serum BUN levels, (B) Cr levels, (C) Urine KIM-1 levels, (D) Urine NGAL levels. n=6, #P<0.01 vs. sham group; $P<0.01 vs. CLP group. miR, microRNA; CLP, cecal ligation and puncture; AKI, acute kidney injury; BUN, blood urea nitrogen; Cr, serum creatinine; KIM-1, kidney injury molecule-1; NGAL, neutrophil gelatinase-associated lipocalin; Ad, adenovirus.

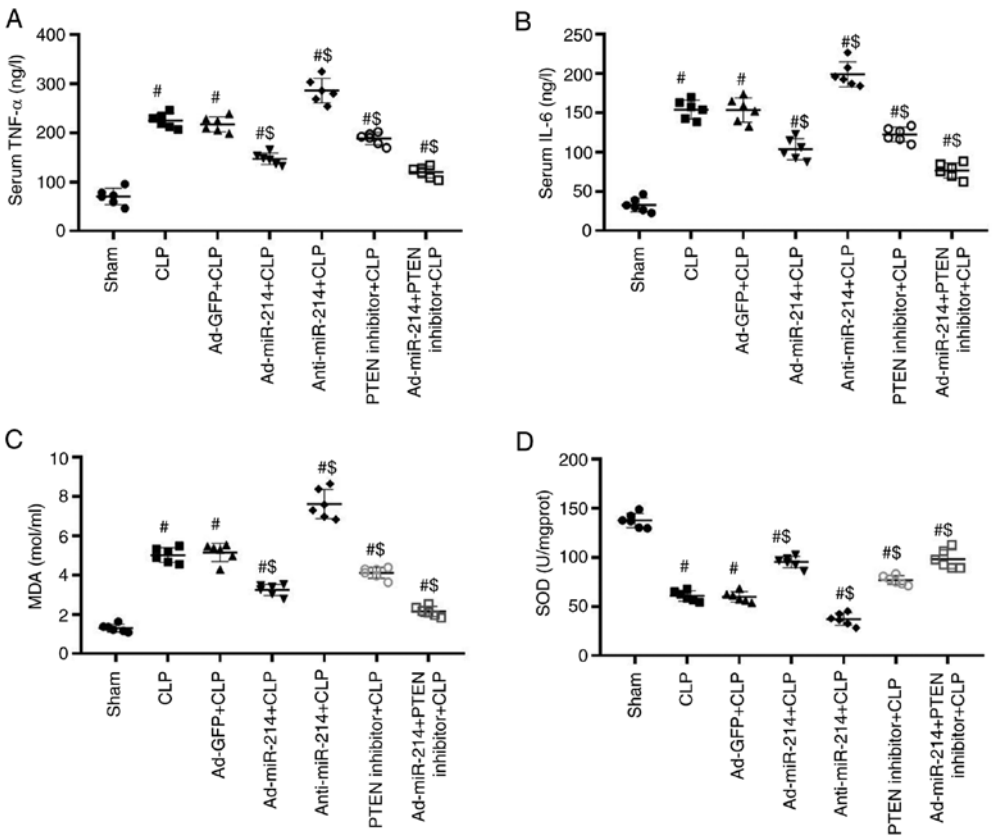

Figure 3. miR-214 reduces inflammation and oxidative stress in CLP-induced AKI. Serum (A) TNF-α and (B) IL-6 levels, (C) MDA concentration and (D) SOD activity. n=6, #P<0.01 vs. sham group; $P<0.01 vs. CLP group. miR, microRNA; CLP, cecal ligation and puncture; AKI, acute kidney injury; MDA, malondialdehyde; SOD, superoxide dismutase; Ad, adenovirus.

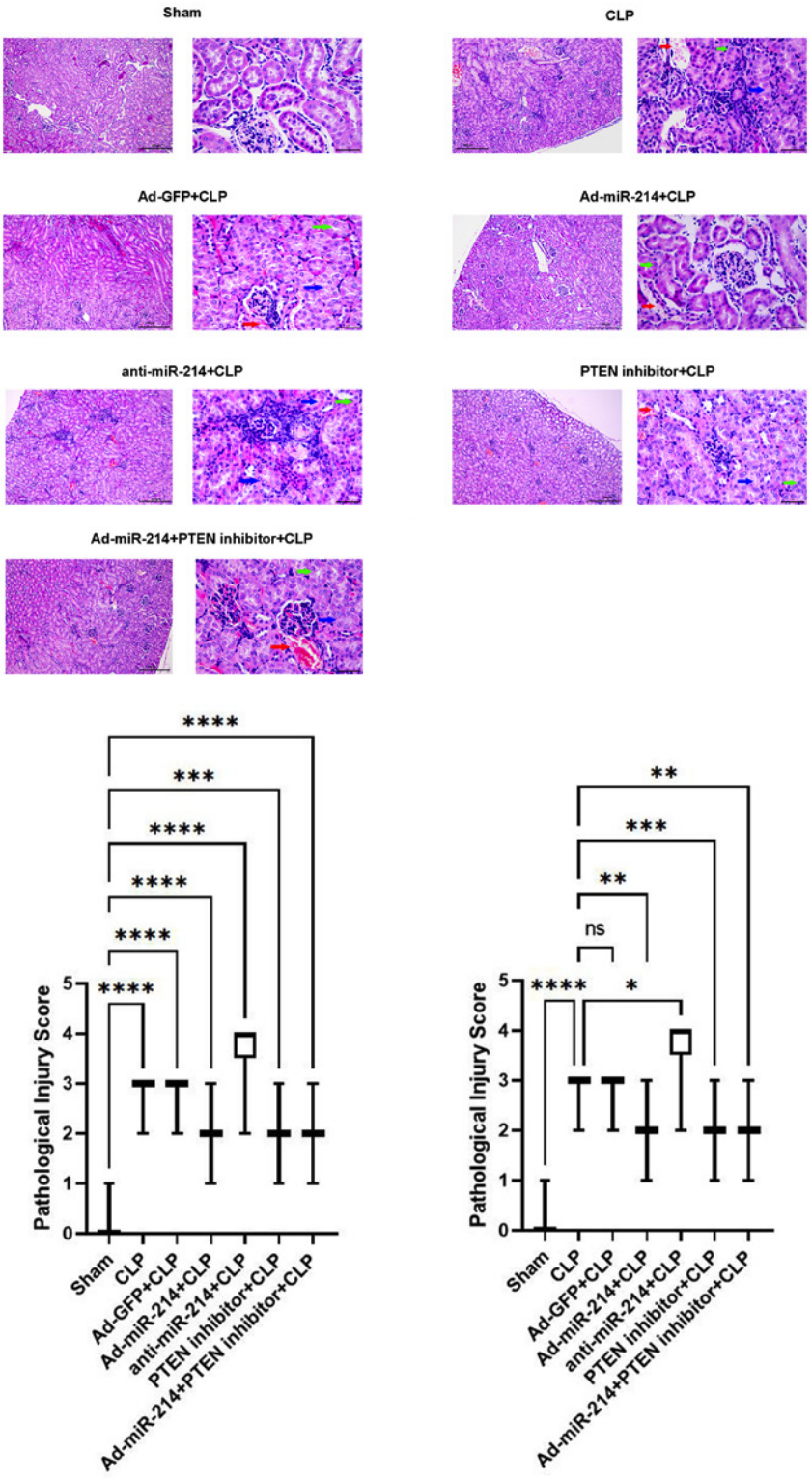

Figure 4. miR-214 attenuates renal histopathological damage. Histological changes in the kidney tissues at 24 h post-CLP (hematoxylin-eosin). Green arrow indicates edema of renal tubular epithelial cells; blue arrow indicates tubular necrosis; red arrow indicates hemorrhage. Magnification, x400, scale bar, 50 μm; x100, scale bar, 100 μm. Semiquantitative histopathological score of injury. n=6, (Kidney pathological images of each mouse were randomly selected from 5 fields), *P<0.05, **P<0.01, ***P<0.001, ****P<0.0001 vs. the sham group and CLP group. miR, microRNA; CLP, cecal ligation and puncture; Ad, adenovirus.

inhibitor and Ad-miR-214 + PTEN inhibitor groups displayed decreased mRNA expression of LC3 and PTEN, but increased mRNA expression of p62, AKT and mTOR (all P<0.05); in the anti-miR-214 group, an opposite changing tendency was observed (all P<0.05). There was no significant difference in the above indicators among the Ad-miR-214 group, the PTEN inhibitor group and the Ad-miR-214 + PTEN inhibitor group (all P>0.05). Thus, the effect of p62 on autophagy may occur at the transcriptional level rather than at the post-transcriptional level. The current results demonstrated that miR-214 downregulated the expression of PTEN and activated the AKT/mTOR signaling pathway.

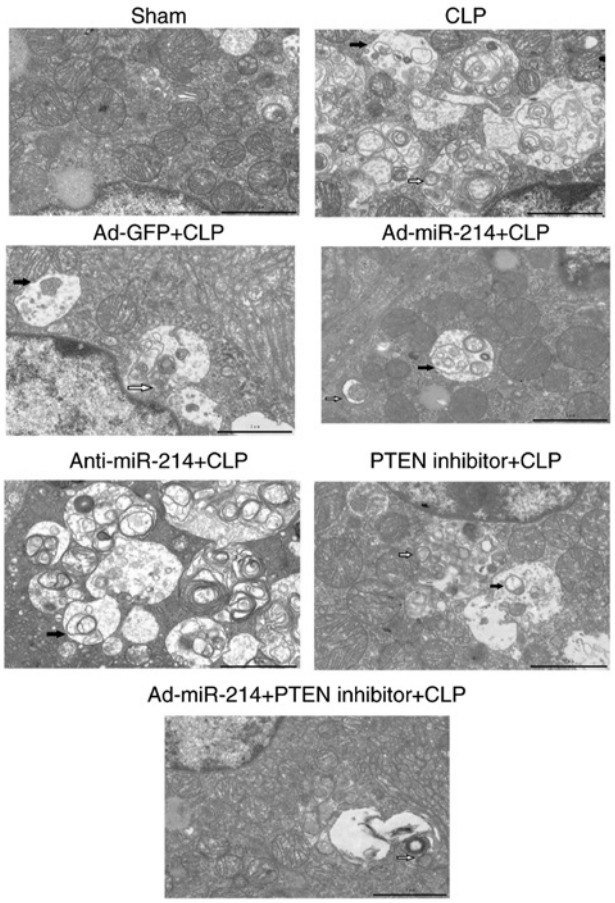

Figure 5. miR-214 attenuates renal ultrastructural changes. Images of electron microscopy of the proximal convoluted tubule of kidney at 24 h after surgery. White arrow heads identify complex structures bounded by two membranes (autophagosomes); black arrow heads identify single membrane-bound lysosomal complexes with degraded organellar content (autolysosomes). n=6. Magnification, x7,000, scale bar, 2 μm. Ad, adenovirus CLP, cecal ligation and puncture; miR, microRNA.

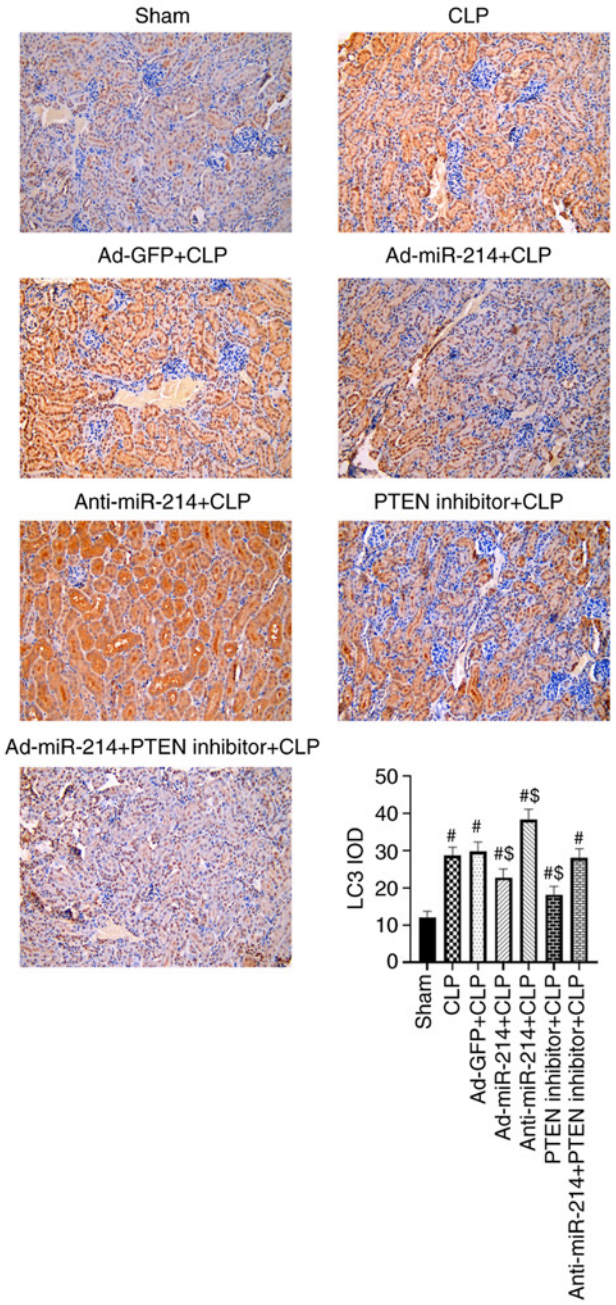

Figure 6. miR-214 attenuates renal autophagy. Immunohistochemistry expression of LC3 was quantified by integral optical density (x200). Scale bar, 50 μm. n=6. $^{\#}$P<0.01 vs. sham group; $^{\$}$P<0.01 vs. CLP group. miR, microRNA; Ad, adenovirus CLP, cecal ligation and puncture.

Discussion

The present study found that excessive autophagy was detrimental to renal function in septic mice. Previous studies have shown that miR-214 is associated with increased proliferation, metastasis, invasion and functions as an oncogene for cells and tissues (19-22). Studies report that miR-214 serves a protective role against AKI via attenuating apoptosis, oxidative stress and downregulating inflammatory factors (21,23). The present study further examined the mechanisms underlying the protective effect of miR-214 on sepsis-induced AKI by focusing on the potential involvement of miR-214 in the modulation of autophagy.

The results showed that oxidative stress occurred in the kidney following the administration of CLP surgery. Meanwhile, the activation of autophagy occurs in the kidney. Elevated LC3 II/I and the reduction of p62 in the kidney was observed following treatment with CLP surgery. As expected, the overexpression of miR-214 significantly attenuated kidney pathological injuries and kidney dysfunction caused by sepsis. However, the inhibition of miR-214 displayed an opposite tendency to renoprotection. In addition, the protection effect of Ad-miR-214 was enhanced by PTEN inhibitor.

In a septic kidney, excessive inflammation is accompanied by massive increases in the production of ROS and a large number of ROS triggers changes in mitochondrial structure and impairs mitochondrial function, which causes the body to enter a vicious cycle which aggravates kidney damage (24,25). Therefore, oxidative stress may be one of the main pathological mechanisms of sepsis-induced AKI. The present study provided further evidence demonstrating excessive oxidative stress, which was indicated by increased MDA production and reduced SOD activity in the kidney tissues following CLP surgery. Moreover, it was found that the overexpression of miR-214 could protect the kidney against CLP-induced oxidative injury, which is involved in autophagic inhibition. This

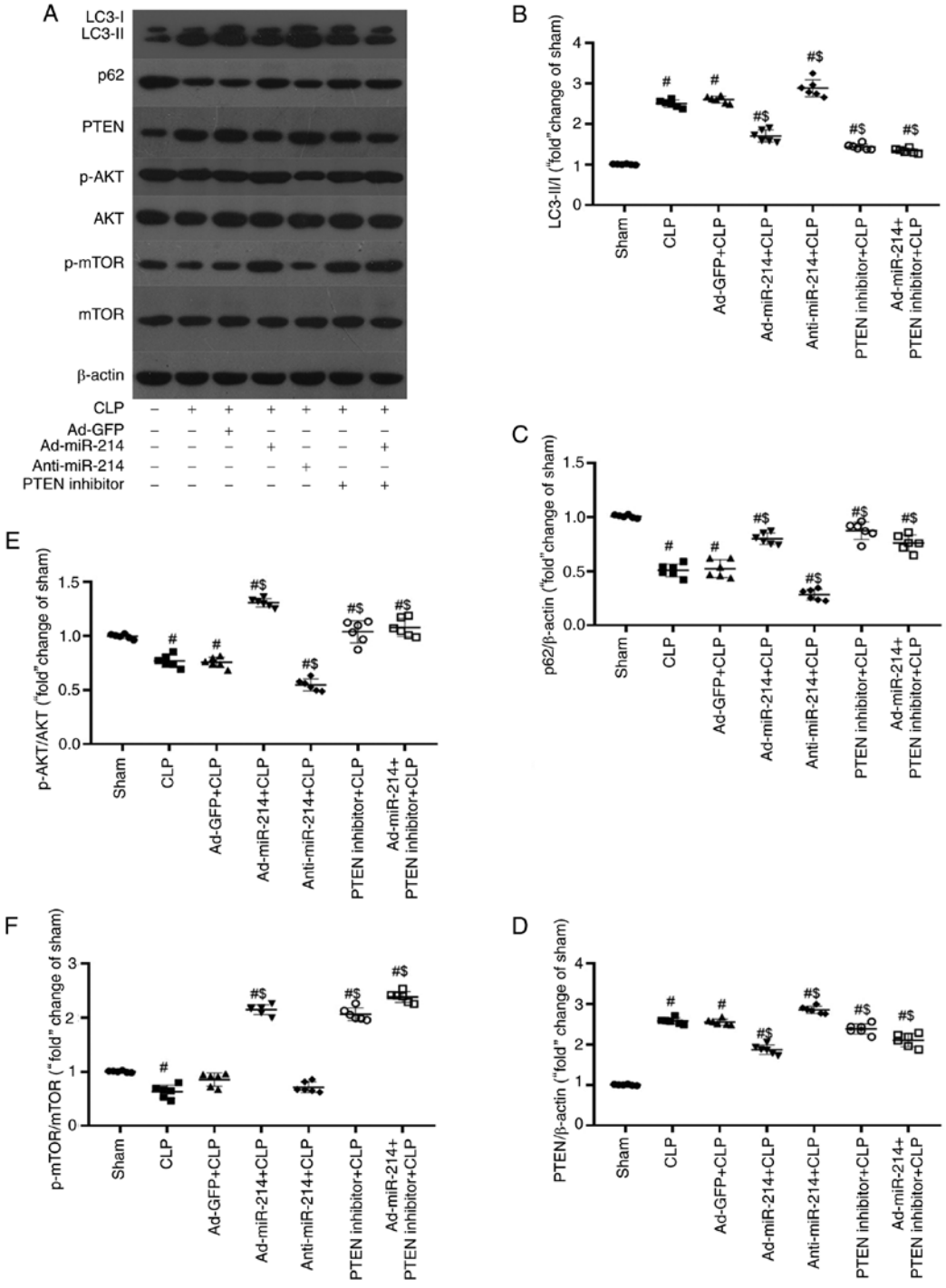

Figure 7. miR-214 inhibits autophagy by regulating the PTEN/AKT/mTOR pathway. miR-214 inhibits renal autophagy and activates autophagy-related AKT/mTOR pathway by silencing PTEN. (A) Representative image of immunoblotting of LC3, p62, PTEN, p-AKT, AKT, p-mTOR, and mTOR with β-actin as loading control. (B and C) Effect of miR-214 on renal autophagy, western blot analyses two autophagy markers LC3-II/I and p62, along with control protein β-actin. (D-F) Effect of miR-214 on the autophagy-related PTEN/AKT/mTOR pathway. n=6, #P<0.01 vs. sham group; $P<0.01 vs. CLP group. miR, microRNA; p-, phosphorylated; Ad, adenovirus CLP, cecal ligation and puncture.

is consistent with the previous studies that miR-214 protects various cells and tissues against oxidative stress (26,27).

Autophagy serves as a 'double-edged sword' in the development of sepsis: Basal autophagy can exert protective effects by removing toxic oxidative proteins, but excessive autophagy may lead to autophagic cellular death under severe stress, such as ROS eruption (28,29). It has been shown that autophagy is activated initially in sepsis, followed by a subsequent phase of dysfunction due to autophagic cell death (30), which aggravates sepsis-induced oxidative injury. In the present study, PTEN inhibitor or overexpression of miR-214 displayed antioxidative renoprotection in CLP-treated mice. However, the inhibition of miR-214 displayed an opposite tendency to antioxidative renoprotection. So excessive or inadequate autophagy can cause kidney damage; both are maladaptive and eventually provoke cell death. Hence, keeping moderate levels of autophagy is the key to attenuate oxidative injury in septic condition.

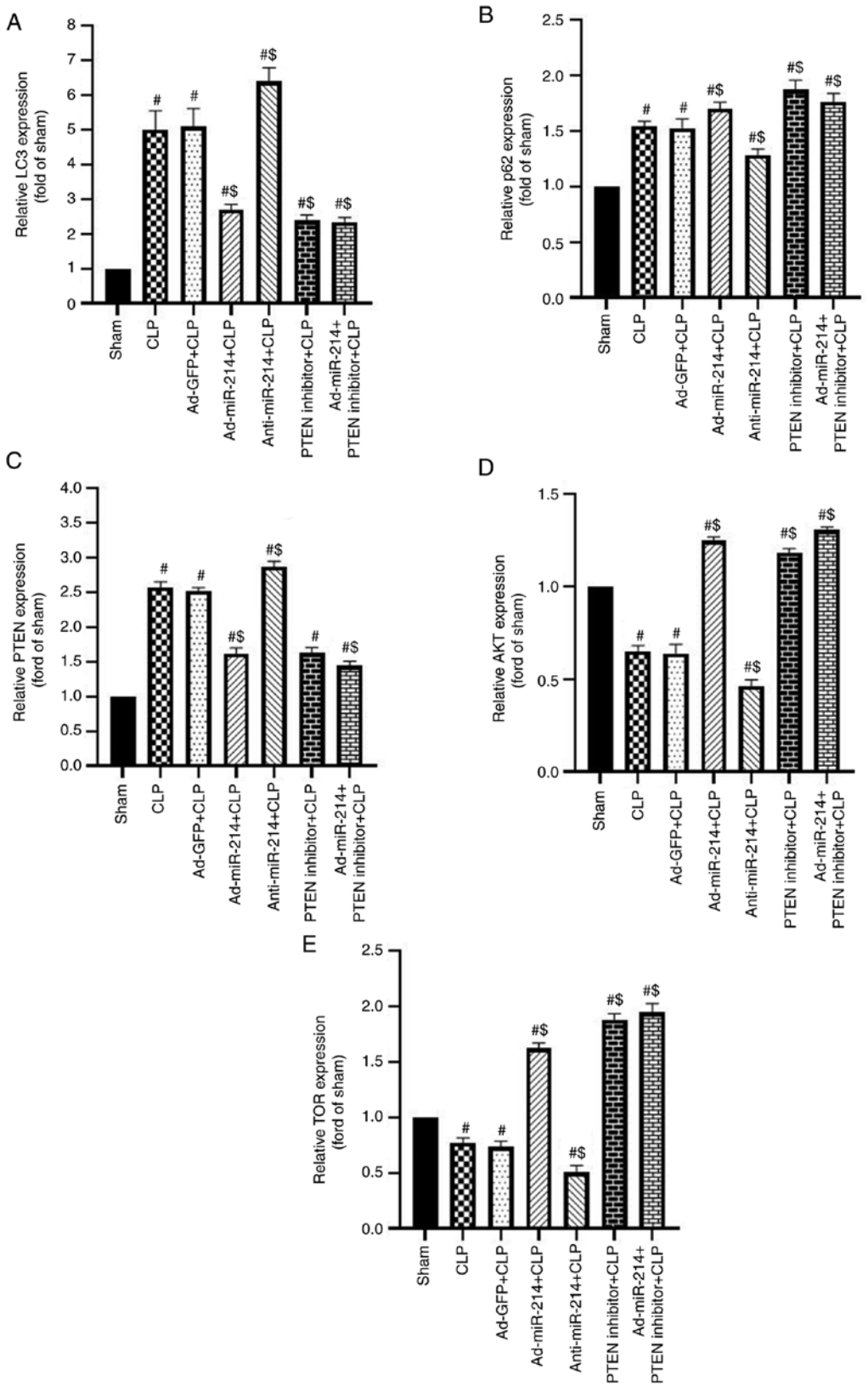

Figure 8. RT-qPCR was further used to determine the expression of mRNA of genes related to the PTEN/AKT/mTOR signaling pathway. (A and B) Effect of miR-214 on renal autophagy, RT-qPCR analyses of two autophagy markers LC3-II/I and p62. (C-E) Effect of miR-214 on the autophagy-related PTEN/AKT/mTOR pathway. n=6. $^{\#}$P<0.01 vs. sham group; $^{\$}$P<0.01 vs. CLP group. miR, microRNA; Ad, adenovirus CLP, cecal ligation and puncture; RT-qPCR, reverse transcription-quantitative PCR.

Accumulating evidence has indicated that miR-214 inhibits autophagy in various cells and tissues (31-33). In the present study, the overexpression of miR-214 was found to inhibit CLP-induced autophagy in kidney tissues, as indicated by the changes in protein markers, such as LC3-II/I and p62. Furthermore, the results demonstrated that

overexpression of miR-214 attenuated CLP-induced oxidative injury by inhibiting excessive autophagy. The present study also investigated the molecular mechanisms by which miR-214 modulates kidney autophagy in sepsis-induced AKI. PTEN/AKT/mTOR is an important signaling pathway that regulates kidney autophagy (34,35) and which serves a key role in sepsis-induced AKI, and PTEN is a negative inhibitor of the PI3K/AKT/mTOR signaling pathway. Previous studies reported that miR-214 can regulate autophagy through the PI3K/AKT/mTOR signaling pathway in various models (36-38). Ma *et al* (39) found that miR-214 can downregulate autophagy in diabetic kidneys. Therefore, it was hypothesized that the effects of miR-214 on CLP-induced AKI might be involved in the regulation of the PTEN/AKT/mTOR pathway. Notably, the results of the present study showed that CLP surgery significantly elevated the levels of PTEN but decreased the levels of p-AKT and p-mTOR, indicating that CLP surgery inactivated the AKT/mTOR pathway. In addition, the overexpression of miR-214 activated the AKT/mTOR pathway by the silencing of PTEN in CLP-induced autophagy in kidney tissues. However, anti-miR-214 did not significantly inhibited the expression of mTOR in western blot analyses. Thus, RT-qPCR was further used to determine the expression of mRNA of genes related to the PTEN/AKT/mTOR signaling pathway. The present study identified that miR-214 downregulated the expression of PTEN and activated the AKT/mTOR signaling pathway to inhibit autophagy. However, further exhaustive studies should be carried out to obtain additional details related to the mechanism of kidney autophagy in septic condition.

To conclude, the results of the present study suggested that miR-214 served a protective role against sepsis-induced kidney injury by reducing oxidative stress and inhibiting autophagy through regulation of the PTEN/AKT/mTOR pathway. The present findings suggested that miR-214 may be a potential therapeutic target for sepsis-induced AKI. However, the present study used mice 6-8 week old, so further research on the mechanism of miR-214 is needed in adult mice.

Acknowledgements

Not applicable.

Funding

No funding was received.

Availability of data and materials

The datasets used and/or analyzed during the current study are available from the corresponding author on reasonable request.

Authors' contributions

ZS and SD contributed conception and design of the study. ZS and YW conducted experiments. ZS and SD organized the database. PZ and ZS performed the statistical analysis. ZS wrote the manuscript. All authors contributed to manuscript revision, read and approved the final version of the manuscript. ZS and SD confirm the authenticity of all the raw data.

Ethics approval and consent to participate

The present study adhered to the Guide for the Care and Use of Laboratory Animals published by the US National Institutes of Health (NIH Publication no. 85-23, revised 1996) and all experimental protocols were approved by the Animal Experimentation Ethics Committee of Cangzhou Central Hospital (approval no. 2017-020-01).

Patient consent for publication

Not applicable.

Competing interests

The authors declare that they have no competing interests.

References

1. Plotnikov EY, Pevzner IB, Zorova LD, Chernikov VP, Prusov AN, Kireev II, Silachev DN, Skulachev VP and Zorov DB: Mitochondrial damage and mitochondria-targeted antioxidant protection in LPS-induced acute kidney injury. Antioxidants (Basel) 8: 176, 2019.
2. Zhang Y, Wang L, Meng L, Cao G and Wu Y: Sirtuin 6 overexpression relieves sepsis-induced acute kidney injury by promoting autophagy. Cell Cycle 18: 425-436, 2019.
3. Zhao W, Zhang L, Chen R, Lu H, Sui M, Zhu Y and Zeng L: SIRT3 protects against acute kidney injury via AMPK/mTOR-regulated autophagy. Front Physiol 9: 1526, 2018.
4. Lelubre C and Vincent JL: Mechanisms and treatment of organ failure in sepsis. Nat Rev Nephrol 7: 417-427, 2018.
5. Greco E, Lupia E, Bosco O, Vizio B and Montrucchio G: Platelets and Multi-Organ failure in sepsis. Int J Mol Sci 18: 2200, 2017.
6. Wu Y, Wang L, Meng L, Cao GK, Zhao YL and Zhang Y: Biological effects of autophagy in mice with sepsis-induced acute kidney injury. Exp Ther Med 17: 316-322, 2019.
7. Yu T, Liu D, Gao M, Yang P, Zhang M, Song F, Zhang X and Liu Y: Dexmedetomidine prevents septic myocardial dysfunction in rats via activation of α7nAChR and PI3K/Akt-mediated autophagy. Biomed Pharmacother 120: 109231, 2019.
8. Hotchkiss RS, Strasser A, McDunn JE and Swanson PE: Cell death. N Engl J Med 361: 1570-1583, 2009.
9. Zhu X, Li W and Li H: miR-214 ameliorates acute kidney injury via targeting DKK3 and activating of Wnt/β-catenin signaling pathway. Biol Res 51: 31, 2018.
10. Yang S, Fei X, Lu Y, Xu B, Ma Y and Wan H: miRNA-214 suppresses oxidative stress in diabetic nephropathy via the ROS/Akt/mTOR signaling pathway and uncoupling protein 2. Exp Ther Med 17: 3530-3538, 2019.
11. Sang Z, Zhang P, Wei Y and Dong S: miR-214-3p Attenuates sepsis-induced myocardial dysfunction in mice by inhibiting autophagy through PTEN/AKT/mTOR Pathway. Biomed Res Int 2020: 1409038, 2020.
12. Takahashi W, Watanabe E, Fujimura L, Watanabe-Takano H, Yoshidome H, Swanson PE, Tokuhisa T, Oda S and Hatano M: Kinetics and protective role of autophagy in a mouse cecal ligation and puncture-induced sepsis. Crit Care 17: R160, 2013.
13. Livak KJ and Schmittgen TD: Analysis of relative gene expression data using real-time quantitative PCR and the 2(-Delta Delta C(T)) method. Methods 25: 402-408, 2001.
14. Tang C, Han H, Yan M, Zhu S, Liu J, Liu Z, He L, Tan J, Liu Y, Liu H, *et al*: PINK1-PRKN/PARK2 pathway of mitophagy is activated to protect against renal ischemia-reperfusion injury. Autophagy 14: 880-897, 2018.
15. Sunahara S, Watanabe E, Hatano M, Swanson PE, Oami T, Fujimura L, Teratake Y, Shimazui T, Lee C and Oda S: Influence of autophagy on acute kidney injury in a murine cecal ligation and puncture sepsis model. Sci Rep 8: 1050, 2018.
16. Zhou RX, Li XH, Qu Y, Li SP and Huang Q: Role of p38 mitogen-activated protein kinase signaling pathway in the hippocampal neurons autophagy of rats with sepsis. Sichuan Da Xue Xue Bao Yi Xue Ban 50: 512-519, 2019 (In Chinese).

17. Vaidya VS, Ozer JS, Dieterle F, Collings FB, Ramirez V, Troth S, Muniappa N, Thudium D, Gerhold D, Holder DJ, *et al*: Kidney injury molecule-1 outperforms traditional biomarkers of kidney injury in preclinical biomarker qualification studies. Nat Biotechnol 5: 478-485, 2010.
18. Lu X, Fan Q, Xu L, Li L, Yue Y, Xu Y, Su Y, Zhang D and Wang L: Ursolic acid attenuates diabetic mesangial cell injury through the up-regulation of autophagy via miRNA-21/PTEN/Akt/mTOR suppression. PLoS One 2: e0117400, 2015.
19. Liu J, Chen W, Zhang H, Liu T and Zhao L: miR-214 targets the PTEN-mediated PI3K/Akt signaling pathway and regulates cell proliferation and apoptosis in ovarian cancer. Oncol Lett 14: 5711-5718, 2017.
20. Gao Y, Fang P, Li WJ, Zhang J, Wang GP, Jiang DF and Chen FP: LncRNA NEAT1 sponges miR-214 to regulate M2 macrophage polarization by regulation of B7-H3 in multiple myeloma. Mol Immunol 117: 20-28, 2020.
21. Yan Z, Zang B, Gong X, Ren J and Wang R: MiR-214-3p exacerbates kidney damages and inflammation induced by hyperlipidemic pancreatitis complicated with acute renal injury. Life Sci 241: 117118, 2020.
22. Yahya SMM and Yahya SMM: The Effect of miR-98 and miR-214 on apoptotic and angiogenic pathways in hepatocellular carcinoma HepG2 cells. Indian J Clin Biochem 35: 353-358, 2020.
23. Yan Y, Ma Z, Zhu J, Zeng M, Liu H and Dong Z: miR-214 represses mitofusin-2 to promote renal tubular apoptosis in ischemic acute kidney injury. Am J Physiol Renal Physiol 318: F878-F887, 2020.
24. Lowes DA, Webster NR, Murphy MP and Galley HF: Antioxidants that protect mitochondria reduce interleukin-6 and oxidative stress, improve mitochondrial function, and reduce biochemical markers of organ dysfunction in a rat model of acute sepsis. Br J Anaesth 110: 472-480, 2013.
25. Yu H, Jin F, Liu D, Shu G, Wang X, Qi J, Sun M, Yang P, Jiang S, Ying X and Du Y: ROS-responsive nano-drug delivery system combining mitochondria-targeting ceria nanoparticles with atorvastatin for acute kidney injury. Theranostics 10: 2342-2357, 2020.
26. Lu XZ, Yang ZH, Zhang HJ, Zhu LL, Mao XL and Yuan Y: MiR-214 protects MC3T3-E1 osteoblasts against H2O2-induced apoptosis by suppressing oxidative stress and targeting ATF4. Eur Rev Med Pharmacol Sci 21: 4762-4770, 2017
27. Wang Y, Zhao R, Liu D, Deng W, Xu G, Liu W, Rong J, Long X, Ge J and Shi B: Exosomes derived from miR-214-enriched bone marrow-derived mesenchymal stem cells regulate oxidative damage in cardiac stem cells by targeting CaMKII. Oxid Med Cell Longev 2018: 4971261, 2018.
28. Decuypere JP, Parys JB and Bultynck G: Regulation of the autophagic bcl-2/beclin 1 interaction. Cells 1: 284-312, 2012.
29. Lei S, Zhang Y, Su W, Zhou L, Xu J and Xia ZY: Remifentanil attenuates lipopolysaccharide-induced oxidative injury by down-regulating PKCβ2 activation and inhibiting autophagy in H9C2 cardiomyocytes. Life Sci 213: 109-115, 2018.
30. Ho J, Yu J, Wong SH, Zhang L, Liu X, Wong WT, Leung CC, Choi G, Wang MH, Gin T, *et al*: Autophagy in sepsis: Degradation into exhaustion? Autophagy 12: 1073-1082, 2016.
31. Zhang Y, Li Q, Liu C, Gao S, Ping H, Wang J and Wang P: MiR-214-3p attenuates cognition defects via the inhibition of autophagy in SAMP8 mouse model of sporadic Alzheimer's disease. Neurotoxicology 56: 139-149, 2016.
32. Yu X, Luo A, Liu Y, Wang S, Li Y, Shi W, Liu Z and Qu X: MiR-214 increases the sensitivity of breast cancer cells to tamoxifen and fulvestrant through inhibition of autophagy. Mol cancer 14: 208, 2015.
33. Wang J, Wang WN, Xu SB, Wu H, Dai B, Jian DD, Yang M, Wu YT, Feng Q, Zhu JH, *et al*: MicroRNA-214-3p: A link between autophagy and endothelial cell dysfunction in atherosclerosis. Acta Physiol (Oxf): Oct 14, 2018 (Epub ahead of print). doi: 10.1111/apha.12973.
34. Li XY, Wang SS, Han Z, Han F, Chang YP, Yang Y, Xue M, Sun B and Chen LM: Triptolide restores autophagy to alleviate diabetic renal fibrosis through the miR-141-3p/PTEN/Akt/mTOR pathway. Mol Ther Nucleic Acids 9: 48-56, 2017.
35. Song N, Zhang T, Xu X, Lu Z, Yu X, Fang Y, Hu J, Jia P, Teng J and Ding X: miR-21 protects against ischemia/reperfusion-induced acute kidney injury by preventing epithelial cell apoptosis and inhibiting dendritic cell maturation. Front Physiol 9: 790, 2018.
36. Wu Q, Shang Y, Shen T, Liu F, Xu Y and Wang H: Neuroprotection of miR-214 against isoflurane-induced neurotoxicity involves the PTEN/PI3K/Akt pathway in human neuroblastoma cell line SH-SY5Y. Arch Biochem Biophys 678: 108181, 2019.
37. Gong L, Xu H, Zhang X, Zhang T, Shi J and Chang H: Oridonin relieves hypoxia-evoked apoptosis and autophagy via modulating microRNA-214 in H9c2 cells. Artif Cells Nanomed Biotechnol 47: 2585-2592, 2019.
38. Liu M, Li Z, Liang B, Li L, Liu S, Tan W, Long J, Tang F, Chu C and Yang J: Hydrogen sulfide ameliorates rat myocardial fibrosis induced by thyroxine through PI3K/AKT signaling pathway. Endocr J 65: 769-781, 2018.
39. Ma Z, Li L, Livingston MJ, Zhang D, Mi Q, Zhang M, Ding HF, Huo Y, Mei C and Dong Z: p53/microRNA-214/ULK1 axis impairs renal tubular autophagy in diabetic kidney disease. J Clin Invest 130: 5011-5026, 2020.